J. Phys.: Condens. Matter **20** (2008) 215203 (7pp) doi:10.1088/0953-8984/20/21/215203

Relaxation of the electrical resistivity in Cr-doped $Nd_{0.5}Ca_{0.5}MnO_3$ single crystals

A S Carneiro[1,2], F C Fonseca[3], T Kimura[4] and R F Jardim[1]

[1] Instituto de Física, Universidade de São Paulo, CP 66318, 05315-970, São Paulo, Brazil
[2] Departamento de Física, Universidade de Federal de Goiás-Campus de Catalão, CP 56, 75704-020, Catalão, Brazil
[3] Instituto de Pesquisas Energéticas e Nucleares, CP 11049, 05422-970, São Paulo, SP, Brazil
[4] Division of Materials Physics, Graduate School of Engineering Science, Osaka University, Toyonaka, Osaka 560-8531, Japan

E-mail: rjardim@if.usp.br

Received 28 December 2007, in final form 25 March 2008
Published 18 April 2008
Online at stacks.iop.org/JPhysCM/20/215203

Abstract

We have performed a systematic study of the time and temperature dependencies of the electrical resistivity ($\rho(T, t)$) in $Nd_{0.5}Ca_{0.5}Mn_{1-x}Cr_xO_3$ single crystals with $x = 0.02$ and 0.07 in order to examine the dynamics of the phase separation. The relaxation effects can be described by the combination of a rapid exponential increase/decrease with a slower logarithmic contribution at longer times. The experimental results suggest the existence of a large temperature window in which huge relaxation effects occur, and the relative fraction of the coexisting phases rapidly changes as a function of time, depending on the initial magnetic state of the sample. The $\rho(T, t)$ relaxation measurements were shown to be a suitable tool for probing the dynamical nature of the phase separation, in which magnetically distinct phases compete against each other in a wide temperature range. In addition, the features observed in the $\rho(T, t)$ curves were found to be in excellent agreement with both the magnetic properties and the structural transitions observed in these manganites.

(Some figures in this article are in colour only in the electronic version)

1. Introduction

Mixed-valence manganites have been the focus of considerable research efforts over recent years in view of the variety of physical phenomena they display such as charge, spin, and orbital ordering, as well as their technological potential in magnetic devices [1, 2]. Nevertheless, one of the most intriguing properties in these compounds is the phase-separated (PS) state with simultaneous coexistence of mesoscopic (submicrometer) ferromagnetic metallic (FMM) and antiferromagnetic (AFM) charge and orbital ordered (CO/OO) insulating domains [3]. The PS state has its origin in the unusual proximity of the free energies of the very distinct ferromagnetic (FM) and CO/OO states, and the fact that the competition between both phases is resolved in mesoscopic length scales, giving rise to real-space inhomogeneities within the material [4]. In fact, both microscopic (nanometer) and mesoscopic scale phase coexistence have been observed experimentally [5, 6]. In addition, intrinsic inhomogeneities caused by the chemical-doping process are also known to alter the physical properties near the phase boundary [7]. Several experimental results indicated that the insulating phase in manganites can be driven to the metallic phase at low temperatures by the application of magnetic field H [8], pressure P [9], high-power laser irradiation [10], and electric field E or excitation current I [11], corroborating the PS scenario. Thus, the PS state, along with the percolation of conducting paths, provides a static picture for the colossal magnetoresistance (CMR) effect, where a resistance network model is controlled by parameters such as H and T. In addition to this, evidence of dynamic fluctuations has been reported, bringing up the need to take into account thermal and quantum fluctuations near the phase boundary [7].

The competition between coexisting phases opens up the possibility for the appearance of interesting time-dependent effects, which may cause a strong influence on the physical properties of a system that displays PS [12–18]. Within this context, relaxation measurements performed on manganites

have revealed a state of dynamic phase separation with the growth of one phase to the detriment of the other. For example, Anane *et al* [13] reported that the magnetic field H driven by metallic state in $Pr_{0.67}Ca_{0.33}MnO_3$ is unstable. The electrical resistivity jumps abruptly, at a given temperature, from low to high values at a particular time after the removal of H. The transition in this compound is isothermal, involving the growth of the insulating phase as a function of time in the FMM state. More recently, transmission electron microscopy imaging (TEM) and electrical resistivity relaxation experiments on $La_{0.23}Ca_{0.77}MnO_3$ showed the existence of a dynamical competition between different phases [19]. These measurements have revealed the growth of the volume fraction of the FM phase against the CO insulating phase. It was argued that this dynamic behavior appears to be linked to magnetic transitions occurring in the compound, suggesting important magnetoelastic effects. The dynamic competition between different phases results from the heterogeneous nature of the ground state in these compounds, and the fluctuations are enhanced near the phase boundary where two or more orderings compete [7]. Nevertheless, a clear understanding of some basic macroscopic signatures of the PS state, including its dynamical behavior, is still lacking, and the true nature of this state is yet to be unveiled.

Among the various mixed-valence manganites studied so far, the $Nd_{0.5}Ca_{0.5}Mn_{1-x}Cr_xO_3$ ($0.00 \leqslant x \leqslant 0.07$) system is of great interest because of the strong competition between the CO/OO and FM states. On cooling from room temperature, the pristine compound $Nd_{0.5}Ca_{0.5}MnO_3$ first enters into a CO/OO state below $T_{CO} \sim 240$ K and then becomes a CE-type long-range ordered AFM below $T_N \sim 170$ K. A few per cent of Cr substitution induces a FMM phase at lower temperatures $T_{MI} \sim 150$ K and suppresses the CO/OO state [20, 21]. Recently, analysis of electron microscopy and other spectroscopic data added evidence for the appearance of various structural phase transitions in this series. Neutron powder diffraction studies on samples with Cr content $x = 0.03$, performed upon cooling, indicated a structural phase transition occurring close to 210 K, where two kinds of perovskite phases have been observed [22]. Also, TEM, electron, and x-ray diffraction experiments have demonstrated the presence of an incommensurate (IC) to commensurate (C) structural phase transition in this Cr-doped manganite [6, 23]. The features displayed by the Cr-doped NdCaMnO series support this material as a prototype manganite for the study of macroscopic properties arising from microscopic competition of different orders.

Here we focus our attention on the dynamic properties of the coexisting phases in manganites displaying the PS state and report the relaxation behavior of the electrical resistivity ($\rho(t)$) in Cr-doped $Nd_{0.5}Ca_{0.5}Mn_{1-x}Cr_xO_3$ single crystals without applying an external magnetic field H. Due to the small energy barriers and strains between the coexisting FM and CO-AFM states, the system can change easily between both states close to the metal–insulator (MI) transition temperature. Within this scenario, we have found that time relaxation measurements are suitable in order to reveal the equilibrium ground state. Our results suggest the existence of a large temperature window in which huge relaxation effects occur, and the relative fraction of the coexisting phases rapidly changes as a function of time.

2. Experimental details

$Nd_{0.5}Ca_{0.5}Mn_{1-x}Cr_xO_3$ ($x = 0.02$, 0.04, and 0.07) crystals were grown by the floating zone method and further details are described elsewhere [8]. Four-wire dc electrical resistivity $\rho(T)$ and isothermal resistivity relaxation $\rho(t)$ measurements were performed between 10 and 300 K by using a linear research resistance bridge with low applied excitation current (~10 μA). The magnetization $M(T)$ measurements, under $H = 100$ Oe, were performed using a superconducting quantum interference device (SQUID) magnetometer from Quantum Design, which was also used as the temperature controller for the $\rho(T, t)$ measurements. A heating/cooling rate of 10 K min^{-1} was set to the desired measuring temperature, and the $M(T)$ data were collected after temperature stabilization at an effective rate of ~4 K min^{-1}. The $\rho(T)$ measurements were performed on both cooling and warming runs with a 5 K min^{-1} rate. In order to assure that the relaxation curves were taken at constant temperature and similar thermal history the $\rho(t)$ data were measured by following the steps: (1) the samples were first cooled from room temperature down to the desired temperature with a slow rate of 3 K min^{-1} in the absence of both electrical current and H; (2) after the measuring temperature was reached and stabilized by the temperature control of the SQUID, an additional delay of $t = 100$ s was waited before the ρ versus time ($t = 0$) curve was recorded; and (3) $\rho(T, t)$ data were taken along ~4 h and this procedure was repeated for several T between 300 and 75 K.

3. Results and discussion

Here, we will concentrate on the experimental results obtained in single crystals with $x = 0.02$ and 0.07. Figures 1(a) and (b) display the temperature dependence of the magnetic susceptibility $\chi(T)$ and the electrical resistivity $\rho(T)$ for both single crystals, respectively. The transition from the paramagnetic PM state to the CO regime is inferred from a subtle change in the slope of $d\rho/dT$ and a large cusp in the $\chi(T)$ data at $T_{CO} \sim 240$ K, as shown in figure 1(a). With decreasing temperature, the $\rho(T)$ curve exhibits a further increase from $T < T_{CO}$ down to $T \sim 60$ K, where a change from insulating ($d\rho/dT < 0$) to metal-like behavior ($d\rho/dT > 0$) takes place. In addition to these features, a clear thermal irreversibility in the $\rho(T)$ data, between cooling and warming runs, is observed below $T \leqslant 210$ K.

The $\chi(T)$ curves taken in ZFC and FC modes are coincident from 300 down to ~210 K. Within this temperature interval a large peak at ~240 K identifies the transition to the CO regime. In addition to this, the $\chi(T)$ curves (ZFC and FC modes) separate each other below $T \sim 210$ K, a behavior that has its counterpart in the $\rho(T)$ curve. A shoulder at a lower temperature $T_N \sim 170$ K is identified in the FC curve as the temperature where long-range AFM order occurs,

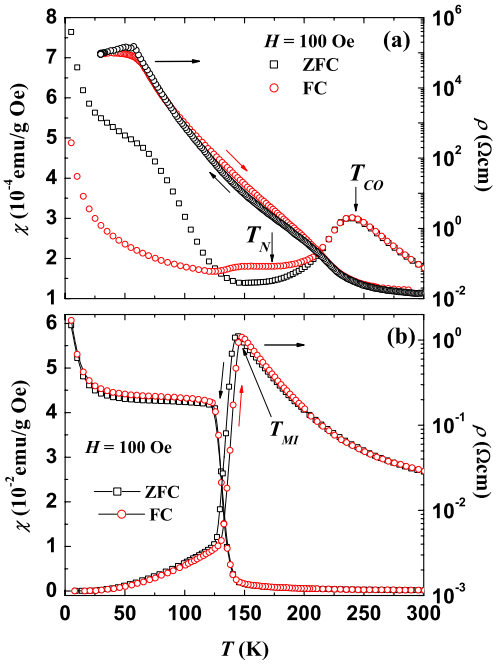

Figure 1. Temperature dependence of the magnetic susceptibility χ (left axis) and the electrical resistivity ρ (right axis) measured in ZFC (squares) and FC (circles) modes of $Nd_{0.5}Ca_{0.5}Mn_{1-x}Cr_xO_3$ with: (a) $x = 0.02$ and (b) $x = 0.07$. Warming and cooling cycles in $\rho(T)$ measurements are indicated by the arrows.

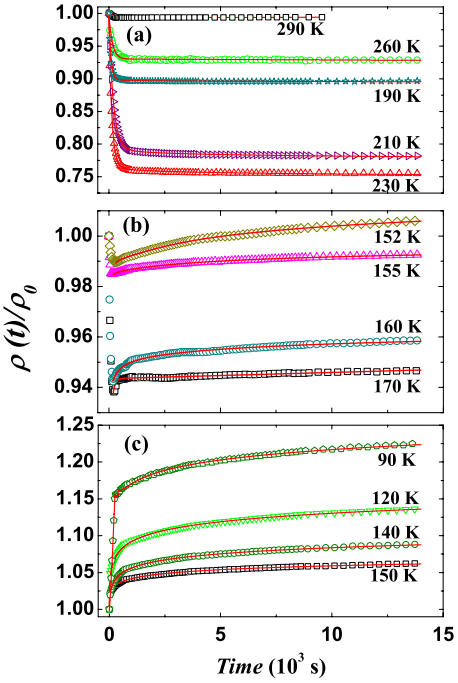

Figure 2. Relative variation of the electrical resistivity of $Nd_{0.5}Ca_{0.5}Mn_{0.98}Cr_{0.02}O_3$ as a function of the time for different temperatures. ρ_0 is the electrical resistivity measured at $t \sim 100$ s, which is assumed here to be $t = 0$. The solid lines are the best fittings using equation (1).

in excellent agreement with neutron diffraction data [8, 21]. An appreciable increase of $\chi(T)$ is observed for temperatures below 50 K and it is ascribed to either a ferromagnetic ordering of the system or to a magnetic contribution due to the Nd sublattice [21]. For single crystals with $x = 0.07$ (figure 1(b)), the quenching of the CO/OO state, which is closely related to the FM transition, occurs at $T_C = 145$ K and is accompanied by a fairly sharp metal–insulator (MI) transition in $\rho(T)$ at the T_{MI}. The thermal irreversibility in both $\chi(T)$ and $\rho(T)$ data indicate a coexistence of CO/OO and FM-metallic phases at low T [8, 14]. Indeed, under Cr-doping and for $T < T_{MI}$ these compounds are comprised of a fine mixture of 20–30 nm nanodomains of the FMM phase embedded in the CO/OO matrix, as inferred from Lorentz microscopy [24].

In order to gain further insight into the properties of these manganites we have measured the long-time relaxation of the electrical resistivity $\rho(T, t)$ in a timescale over 10^4 s. Figure 2 displays the normalized $\rho(t)/\rho_0$ data versus time, where ρ_0 is the first measurement considering the initial $t = 0$ (after a waiting time $t \sim 100$ s), for a single crystal with $x = 0.02$. Generally, the time relaxation of the electrical resistivity varies between two different regimes, depending on the measuring temperature. In fact, the $\rho(t)/\rho_0$ was found to decrease/increase quickly in short times ($t < 300$ s) at all temperatures. On the other hand, for longer timescales $\rho(t > 10^3)/\rho_0$ changes smoothly with increasing time.

Starting from high temperatures, the results of figure 2(a) show that the electrical resistivity of the system decreases monotonically with increasing t, i.e. $\rho(t)/\rho_0 < 1$ for $290 < T < 230$ K. Close to room temperature, $T = 290$ K, a small decrease of ∼1% in $\rho(t)$ is observed. The data also indicate that, in this T range, the saturation values of $\rho(t > 10^3\ \text{s})/\rho_0$ first decrease with decreasing temperature, reaching a minimum value at $T \sim 230$ K. In fact, at $T \sim 230$ K the compound exhibits a pronounced relaxation, corresponding to a maximum decrease of ∼25% of the ρ_0, while for both higher and lower T the relaxation is less pronounced. These results indicate the existence of a negative electrical resistivity relaxation at temperatures where no or negligible short-range FM ordering is present within the material. As T decreases, the saturation $\rho(t)/\rho_0$ continuously increases in magnitude for the curves taken at 210 and 190 K, indicating that the minimum at $T \sim 230$ K is certainly related to the transition of the system to the CO state.

The data of figure 2(b) indicate that further decreasing T, from 170 K down to 152 K, results in a drastic change of the time dependence of $\rho(t)/\rho_0$. In this temperature range, a much less pronounced relaxation is observed (<5%) and the data clearly show that $\rho(t)$ first decreases rapidly up to $t \sim 100$ s, and then the relaxation behavior changes to a slowly increasing behavior with increasing time. Such an increase of $\rho(t)$ is certainly related to the onset of spin ordering taking place at $T_N \sim 170$ K. The non-monotonic behavior of $\rho(t)/\rho_0$ in this temperature range continuously evolves as the measuring temperature decreases and is qualitatively different from the curves measured at $T \gtrsim 190$ K and $T \lesssim 150$ K (see figure 2(c)). Surprisingly, upon decreasing T, we have found a critical temperature $T_{CR} \sim 150$ K below which the initial decrease of $\rho(t)/\rho_0$ is absent, the relaxation reverses its trend, and displays saturation values $\rho(t)/\rho_0 > 1$, as inferred

from the data of figure 2(c). The ratio $\rho(t)/\rho_0$ systematically increases with decreasing temperature: from ∼6% at 150 K up to ∼22% at 90 K.

It is also important to notice that the sign change of the relaxation, which was found to occur at $T_{CR} \sim 150$ K, coincides with the temperature interval ∼130–150 K where a rapid change in the structural parameters has been reported in similar compounds [6, 23]. In fact, low-T transmission electron microscopy (TEM) studies revealed that the $Nd_{0.5}Ca_{0.5}Mn_{1-x}Cr_xO_3$, with $0.02 \leqslant x \leqslant 0.06$, single crystals have an inhomogeneous microstructure comprised of 20–50 nm domains for $T < T_{CO}$. In addition, an incommensurate-to-commensurate (IC–C) type CO phase transition at $T_{IC-C} \sim 130$–150 K in the $x = 0.02$ single crystals was observed [6]. Below T_{IC-C}, the $x = 0.02$ specimen was found to exhibit long-range ordered commensurate CO domains with sizes larger than 100 nm. Short-range ordered incommensurate CO domains, comprised of a fine mixture of nanometer-sized CO and FM clusters, were also observed to exist at $T > T_{IC-C}$ for compounds with $x = 0.02$ and over the whole T range investigated for compounds with higher Cr-doping [6, 23].

The experimental data of figure 2 indicate that the increase of the electrical resistivity with time takes place below $T_N \sim 170$ K, where the AFM ordering occurs [21]. Similar increase of $\rho(t)$ below $T_N \sim 150$ K has been observed in the insulating compound $Nd_{0.5}Ca_{0.5-y}Sr_yMnO_3$ with $y = 0.08$ [25]. Due to these features, it is then reasonable to correlate changes in the $\rho(t)$ relaxation behavior to the occurrence of the CO/OO state below T_{CO}, induced by the CE-type AFM ordering. Besides this, a careful inspection of the FC $\chi(T)$ curve (see figure 1(a)) indicates an anomalous behavior at $T \sim T_{CR} \sim 150$ K, a feature probably related to the phase transition occurring at T_{IC-C}. Such an anomaly in $\chi(T)$ is certainly associated with the decrease of the volume fraction of the short-range FM domains against the growth of the long-range ordered CO state below T_{IC-C} [25].

To gain further insight into the coexistence and phase competition in these systems, we have measured the relaxation of $\rho(t)$ in a crystal with $x = 0.07$ which exhibits a well-pronounced MI transition. The relevant results of the electrical resistivity relaxation of a single crystal of $Nd_{0.5}Ca_{0.5}Mn_{0.93}Cr_{0.07}O_3$ are displayed in figure 3. The data of figure 3(a) shows that in the 300–175 K range $\rho(t)/\rho_0$ is always <1. The absence of changes in the relaxation behavior close to $T_{CO} \sim 240$ K strongly indicates that increasing Cr-doping to $x = 0.07$ results in the complete suppression of the CO state. At high temperatures, the relaxation increases with decreasing temperature and the saturation value $\rho(t > 10^3\ \text{s})/\rho_0$ exhibits a minimum at ∼175 K. For $T < 175$ K, the system changes to a more resistive state as $\rho(t)/\rho_0 \rightarrow 1$ and curves taken with decreasing T continuously show a less pronounced time dependence of $\rho(t)$. Such a feature is certainly related to the AFM ordering expected to occur at $T_N \sim 170$ K. As T further decreases, the relaxation curves measured between 144 and 146 K (figure 3(b)) display a reversal of the relaxation ($\rho(t)/\rho_0 > 1$). Such a relaxation reversal occurs at T close to $T_{CR} \sim T_{MI}$. The curves

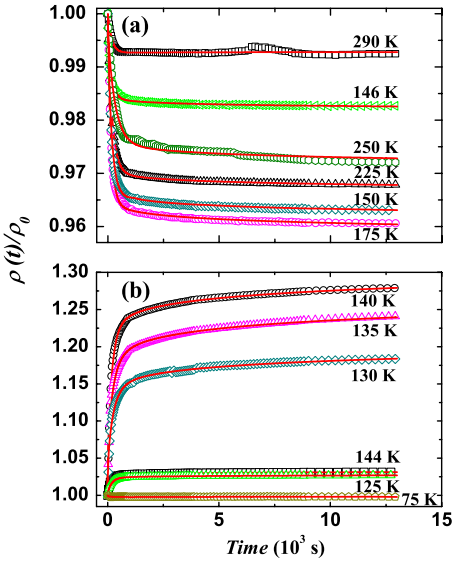

Figure 3. Normalized isothermal electrical resistivity relaxation versus time of $Nd_{0.5}Ca_{0.5}Mn_{0.93}Cr_{0.07}O_3$ at several temperatures. The solid lines are the fittings performed using equation (1).

taken at $T < T_{MI}$ exhibit $\rho(t)/\rho_0 > 1$, as displayed in figure 3(b). In the insulating state $T > T_{MI}$, the absolute variation of the electrical resistivity has a maximum of ∼4% at ∼175 K. The reversal to a positive relaxation in the metallic state results in a much more pronounced time dependence of $\rho(t)$ which reaches an absolute variation of ∼28% at ∼140 K. Such a time dependence decreases for temperatures well below the MI transition and the $\rho(t)$ data measured at 75 K were roughly constant for more than 10^4 s, a behavior consistent with the increasing volume fraction of the metallic phase with decreasing T. A linear time dependence of ρ in $La_{0.9}Sr_{0.1}MnO_3$ ultrathin films has been reported recently by Chen *et al* [18]. Similarly, they have observed relaxation of the electrical resistivity in both the insulating and metallic states with opposite relaxation rates and a change of sign across the MI transition, driven by both temperature and magnetic field.

In the present study, the time relaxation of $\rho(t)$ has been observed in a wide range of temperature in samples displaying both metallic and insulator behaviors. The relaxation data of $\rho(t)$ indicate that when the insulating phase dominates the system evolves to a more conducting state and vice versa. Such a behavior evidences that both FMM and AFM phases compete each other in a large T range, and further suggest that the $\rho(T)$ data shown in figures 1(a) and (b) do not correspond to the response of a system in a true thermodynamic equilibrium. In order to discuss quantitatively the above-mentioned changes in the relaxation of the $\rho(t)$ data, we have fitted the temporal evolution of the electrical resistivity $\rho(t)/\rho_0$ to a phenomenological model consisting of an exponential function and a logarithmic dependence to account for the long-time behavior, according to the expression:

$$\rho(T,t) = \rho_0 + A\left(1 - \exp\left(\frac{-t}{\tau(T)}\right)\right) + s(T)\ln(t) \qquad (1)$$

where $\rho_0 = 1$ is the initial normalized electrical resistivity, A is a free parameter, τ is the temperature-dependent relaxation

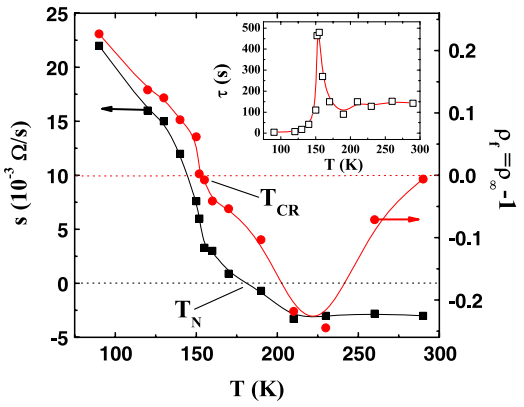

Figure 4. Temperature dependence of the fitting parameters s (left axis) and ρ_f (right axis) defined in equation (1) for the single crystal with $x = 0.02$. Horizontal dotted lines indicate $s = 0$ and $\rho_f = 0$. The inset displays the time relaxation $\tau(T)$ as a function of temperature. The corresponding error bars associated with the fitting procedure are smaller than the symbols used in all cases and the continuous lines are guides to the eye.

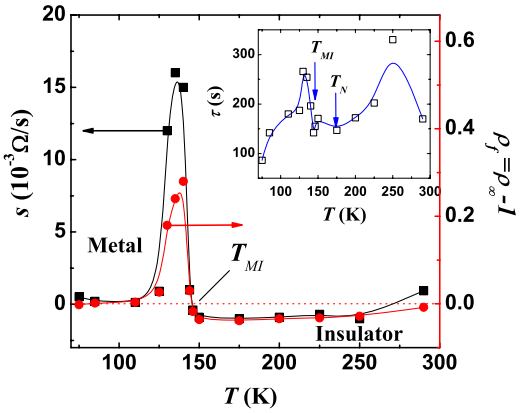

Figure 5. Temperature dependence of the fitting parameters s (left axis) and ρ_f (right axis) for the single crystal with $x = 0.07$. Solid lines are a guide to the eye. The horizontal dotted line indicates $s = 0$ and $\rho_f = 0$. The inset displays the time relaxation $\tau(T)$ as a function of temperature.

time, and s is the resistivity relaxation rate. The solid lines in figures 2 and 3 correspond to the fittings according to the model proposed in equation (1). Generally, equation (1) was able to capture all the relevant changes in the behavior of $\rho(t)/\rho_0$ and a good agreement between the fitting procedure and the experimental data was found, as can be inferred in both figures. The temperature dependence of the fitting parameters s and τ are displayed in figures 4 and 5 for samples with $x = 0.02$ and 0.07, respectively. In addition, both figures also exhibit the temperature dependence of $\rho_f = \rho_\infty - 1$. Here, ρ_∞ is a time-independent background parameter and corresponds to the asymptotic value of $\rho(t)/\rho_0$, when the relaxation time approaches infinity, and the system is believed to achieve thermodynamic equilibrium. The data of figure 4 show that both parameters s and ρ_f decrease monotonically with increasing temperature and change their sign from positive to negative close to the onset of $T_N \sim 170$ K and T_{CR}, respectively. Increasing temperature above ~210 K, results in an almost temperature-independent value of s with a small negative value, while ρ_f exhibits a negative value and an upturn just below T_{CO}.

The parameter s represents here the dynamic behavior of the phase separation, where the competing phases change their volume fraction as a function of time in a given T window. In this scenario, the $s > 0$ behavior for $T < T_N$ is related to the increase of the volume fraction of the CO phase as a function of time. On the other hand, for $T > T_N$, $s < 0$, and reflects the FM phase fraction growth as a function of time.

The relaxation time τ versus T is displayed in the inset of figure 4. This parameter can be interpreted as a measurement of the timescale in which the relaxation process occurs. The typical values obtained for τ, close to 10^2 s, are orders of magnitude larger than the microscopic spin flip times ($\sim 10^{-12}$ s) and even larger than the relaxation times of current densities in superconductors ($\sim 10^{-6}$ s) [26]. However, the most striking behavior is revealed by the comparison of ρ_f and τ at $T_{CR} \sim 150$ K where ρ_f changes its sign and τ displays a pronounced peak. This peak in τ occurs where the energy barriers between the FM and CO-AFM states of the system reaches a minimum value. In addition, similar slow relaxing behavior in a quasi-equilibrium state has been reported in both FM-metallic and CO insulating phases in similar compounds [18, 19], suggesting that such a feature is an intrinsic property of these manganites.

The temperature dependence of the fitting parameters s, τ, and ρ_f for the sample with $x = 0.07$ is displayed in figure 5. Here, both s and ρ_f clearly exhibit a similar temperature dependence. s and ρ_f are positive in the metallic state, and negative in the insulating state $T > T_{MI}$. However, at low temperatures the system is frozen in its phase-separated metallic state, i.e. the volume fraction of the metallic phase is much larger than that of the CO phase at $T \ll T_{MI}$, and $s \approx 0$. With increasing T, both parameters display a pronounced peak at 125 K $\leqslant T \leqslant T_{MI} \sim 150$ K, which is the same T region where a thermal irreversibility is observed in the $\rho(T)$ data (see figure 1). The large relaxation rates s observed at $T \approx T_{MI}$ indicate that the PS is a dynamic process in this series, with the volume fraction of the coexisting phases changing continuously as a function of time, a feature more pronounced in the T-range close to the FMM transition. Interestingly, at temperatures close to but a little above T_{MI} both s and ρ_f are ≈0, indicating that the system experiences a much less intense phase competition. For $T > T_{MI}$, a change from positive to negative in the sign of both s and ρ_f occurs, leading the insulating state to a more conducting one with increasing time. The dynamic behavior is also reflected in the τ dependence on the temperature, as seen in the inset of figure 5. Increasing the temperature from ~80 K results in an increase of τ, which displays a peak in the vicinity of T_{MI}, a region where the competition between phases is severe, as inferred from the high s values. For $T > T_{MI}$, τ exhibits a minimum close to T_N followed by a gradual increase up to T_{CO}, further evidencing the inhomogeneous nature of the CO state.

Our experimental data allowed us to verify that the observed electrical resistivity relaxation can be intimately related

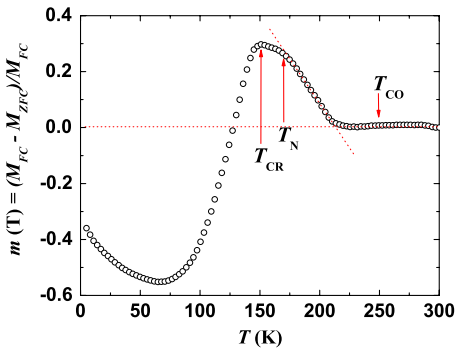

Figure 6. The difference between ZF and ZFC low-field magnetization as a function of temperature for the single crystal with $x = 0.02$.

to the dynamic coexistence of magnetically distinct phases in the PS scenario. In fact, we have attributed the observed instabilities to the competition between the FM-, CO-, and the CE-type OO phases. However, it is important to consider that the electrical resistivity of the phase-separated system not only depends on the relative volume fraction of the coexisting phases, but also on the distribution of the conductive domains, their size, and shape [27]. At the various stages of the percolation of conductive domains, the system could be more insulating or more metallic, as can be inferred from the variety of behaviors observed in the relaxation measurements. Within this context, it is important to notice that the observed temperature dependence of the relaxation parameters is reflected in both magnetic and structural transitions in these Cr-doped manganites.

The observed features of the electrical resistivity relaxation measurements have their counterpart in the magnetic properties. Let us concentrate on the magnetic properties of the sample with $x = 0.02$ where an inhomogeneous ground state occurs in a wider range of temperatures and differences in the magnetic properties are pronounced. Thus, the temperature dependence of the reduced moment, defined as $m(T) = (M_{FC} - M_{ZFC})/M_{FC}$ and shown in figure 6, is helpful to visualize the magnetic regimes of the sample with $x = 0.02$. The $m(T)$ data indicate the existence of four different regimes that have a clear correspondence in the relaxation behavior of the $\rho(t)$ (see figures 1, 2). At high temperatures, as expected for a paramagnetic phase, the reduced moment remains close to $m(T) \sim 0$, a behavior which is consistent with the very small $\rho(t)$ relaxation observed in this T range (see figure 2). On the other hand, the ZFC and FC curves start to deviate from each other below T_{CO} at 210 K, indicating irreversibility below this temperature and the development of magnetic correlations. This suggests either the presence of small domains with short-range FM ordering or inhomogeneities within the CO matrix. In fact, neutron powder diffraction studies on a similar Cr-doped CO/OO manganite [22] indicated that with decreasing temperature below 210 K the system transforms into a two-phase state, consisting of two perovskite structures with different c-axis length, as discussed above. The results shown in figure 4 are also of interest and indicate that the relaxation rate time s increases with decreasing temperature at $T \sim 210$ K, which corresponds exactly to the onset of the splitting between ZFC and FC curves, as displayed in figure 1. Such a feature is mirrored in the $\rho(t)$ relaxation in this T range, where an evolution to a more conducting state ($s < 0$) for $T_N < T < T_{CO}$ is observed. In the latter T interval, the $m(T)$ data can be approximated by a straight line, as indicated in figure 6, and the temperature in which the slope changes is identified as T_N. Below T_N, the long-range OO ordering is established and a more insulating state develops, as indicated by the increasing $\rho(t)$ ($s > 0$) in this T range. At T_{CR}, $m(T)$ reaches a maximum and the observed inflection of $m(T)$ is related to the long-range coherence loss of the FM clusters due to the development of the AFM ordering, associated with the IC–C transition of the CO phase that takes place between 150–130 K [6, 23]. The critical transition temperature $T_{CR} \sim 150$ K, determined from the relaxation data, is in good agreement with the temperature where the difference between ZFC and FC processes is maximum.

4. Conclusion

In summary, we have found, by means of time-dependent electrical resistivity measurements in the inhomogeneous phase-separated Cr-doped $Nd_{0.5}Ca_{0.5}Mn_{1-x}Cr_xO_3$ manganites, that the behavior of $\rho(t)$ changes between two different regimes: (i) a stretched exponential trend, displaying a quick decrease or increase of $\rho(t)$; and (ii) a slow logarithmic decrease or increase as well. Both of them were found to occur in a wide temperature range and to be dependent on the initial magnetic state of the sample. The insulating single crystal ($x = 0.02$) exhibits an unusual temperature dependence of the relaxation curves in the region between $T_N \sim 170$ K and the critical temperature $T_{CR} \sim 150$ K. Much more pronounced relaxation effects along with a reversal of the relaxation trend were observed at temperatures $T \sim T_{CR,CO}$ and $T \sim T_{MI}$ for the insulating charge-ordered compound ($x = 0.02$) and the one displaying a metal–insulator transition ($x = 0.07$), respectively. In addition, the relaxation data clearly reflect the magnetic and structural changes in this series, in excellent agreement with results of both magnetization and neutron diffraction measurements performed in similar single crystals. The electrical resistivity relaxation measurements assure the inhomogeneous nature of the ground state of these compounds, and can be ascribed as a helpful tool for probing the phase dynamics in such manganites. Our results evidence the dynamic behavior of the coexisting phases, including a phase-separated state, characterized by the competition of different magnetic phases in a wide temperature range of both insulating and conducting states of the Cr-doped manganites.

Acknowledgments

This work was supported by the Brazilian agency FAPESP under Grant Nos 05/53241-9 and 01/01454-8. RFJ and FCF are CNPq (Brazil) fellows under Grant Nos 303272/2004-0 and 301661/2004-9, respectively.

References

[1] Ramirez A P 1997 *J. Phys.: Condens. Matter* **9** 8171
[2] Coey J M D, Viret M and von Molnar S 1999 *Adv. Phys.* **48** 167
[3] Dagotto E, Hotta T and Moreo A 2001 *Phys. Rep.* **344** 1
[4] Ghivelder L, Freitas R S, das Virgens M G, Continentino M A, Martinho H, Granja L, Quintero M, Leyva G, Levy P and Parisi F 2004 *Phys. Rev.* B **69** 214414
[5] Zhang L, Israel C, Biswas A, Greene R L and Lozanne A D 2002 *Science* **298** 805
[6] Xu J, Matsui Y, Kimura T and Tokura Y 2001 *Physica* C **357–360** 401
[7] Murakami S and Nagaosa N 2003 *Phys. Rev. Lett.* **90** 197201
[8] Kimura T, Kumai R, Okimoto Y, Tomioka Y and Tokura Y 2000 *Phys. Rev.* B **62** 15021
[9] Moritomo Y, Kuwahara H, Tomioka Y and Tokura Y 1997 *Phys. Rev.* B **55** 7549
[10] Miyano K, Tanaka T, Tomioka Y and Tokura Y 1997 *Phys. Rev. Lett.* **78** 4257
[11] See, for instance Asamitsu A, Tomioka Y, Kuwahara H and Tokura Y 1997 *Nature* **388** 50
Carneiro A S, Jardim R F and Fonseca F C 2006 *Phys. Rev.* B **73** 012410
[12] Babushkina N A, Belova L M, Khomskii D I, Kugel K I, Yu Gorbenko O and Kaul A R 1999 *Phys. Rev.* B **59** 6994
[13] Anane A, Renard J-P, Reversat L, Dupas C, Veillet P, Viret M, Pinsard L and Revcolevschi A 1999 *Phys. Rev.* B **59** 77
[14] Kimura T, Tomioka Y, Kumai R, Okimoto Y and Tokura Y 1999 *Phys. Rev. Lett.* **83** 3940
[15] López J, Lisboa Filho P N, Passos W A C, Ortiz W A, Araujo-Moreira F M, de Lima O F, Schaniel D and Ghosh K 2001 *Phys. Rev.* B **63** 224422
[16] Sirena M, Stern L B and Guimaraes J 2001 *Phys. Rev.* B **68** 104409
[17] Levy P, Parisi F, Quintero M, Granja L, Curiale J, Sacanell J, Leyva G, Polla G, Freitas R S and Ghivelder L 2002 *Phys. Rev.* B **65** 140401
[18] Chen X J, Habermeier H-U and Almasan C C 2003 *Phys. Rev.* B **68** 132407
[19] Tao J, Niebieskikwiat D, Salamon M B and Zuo J M 2005 *Phys. Rev. Lett.* **94** 147206
[20] Carneiro A S, Fonseca F C, Jardim R F and Kimura T 2003 *J. Appl. Phys.* **93** 8074
[21] Schuddinck W, Van Tendeloo G, Barnabé A, Hervieu M and Raveau B 2000 *J. Magn. Magn. Mater.* **211** 105
[22] Moritomo Y, Machida A, Nonobe T and Ohoyama K 2002 *J. Phys. Soc. Japan* **71** 1626
[23] Mori S, Shoji R, Yamamoto N, Machida A, Moritomo Y and Katsufuji T 2002 *J. Phys. Soc. Japan* **71** 1280
[24] Mori S, Shoji R, Yamamoto N, Asaka T, Matsui Y, Machida A, Moritomo Y and Katsufuji T 2003 *Phys. Rev.* B **67** 012403
[25] Chang C W, Debnath A K and Lin J G 2001 *Phys. Rev.* B **65** 024422
[26] Ghivelder L and Parisi F 2005 *Phys. Rev.* B **71** 184425
[27] Khomskii D and Khomskii L 2001 *Phys. Rev.* B **67** 052406